The arrangements of Cr atoms in FCC Au-Cr alloys

1990 J. Phys.: Condens. Matter 2 5647

(http://iopscience.iop.org/0953-8984/2/26/001)

J. Phys.: Condens. Matter 2 (1990) 5647–5653. Printed in the UK

The arrangements of Cr atoms in FCC Au–Cr alloys

Kenji Koga and Ken-ichi Ohshima
Institute of Applied Physics, University of Tsukuba, Tsukuba 305, Japan

Received 12 December 1989, in final form 22 March 1990

Abstract. The intensity of x-ray diffuse scattering was measured at room temperature for FCC Au–Cr alloys whose compositions are 20.2, 12.6 and 8.4 at.% Cr. Diffuse maxima due to atomic short-range order (ASRO) were observed at $1\frac{1}{2}0$ and its equivalent positions for the three specimens, while their intensities decrease with decreasing Cr content. From computer-simulated arrangements of Cr atoms in a FCC lattice, based on the observed ASRO parameters, the Cr atoms were found to have a preference for lining up along the $\langle 1\,0\,0\rangle$ direction for the Au–20.2 at.% Cr alloy. On the other hand, the Cr atoms tend to have random positions for the Au–8.4 at.% Cr alloy and have an intermediate arrangement for the Au–12.6 at.% Cr alloy. The relationship between the ASRO state and the magnetic property in FCC Au–Cr alloys is discussed.

1. Introduction

Noble-metal alloys containing 3d transition metals show spin-glass behaviour at low temperatures when their compositions are less than about 15 at.%. Though theoretical and experimental studies have been performed widely to establish the microscopic description of the spin system in real space, the overall ideas are not clear yet. Neutron scattering studies provide us with information about both local atom and spin arrangements in the alloys while x-ray studies only provide an insight into the local atom arrangement through the analysis of diffuse intensity data. However, it is still of fundamental importance to have such structural information from x-ray diffuse scattering in order to understand the magnetic aspects based on the spin configuration. In previous papers (Suzuki *et al* 1982, Ohshima *et al* 1987) it has been pointed out from analysing x-ray diffuse scattering data that the magnetic properties have a strong relation to the local atomic arrangements of Mn atoms in FCC Au-based binary alloys. In order to understand the spin-glass state of noble-metal alloys containing 3d transition metals, we have to extend the x-ray diffraction studies to another alloy system. We have thus chosen the FCC Au–Cr alloy system.

The magnetic phase diagram of FCC Au–Cr alloys has been constructed by Nakai *et al* (1987) with the use of magnetic and neutron diffraction measurements. They show that spin-glass behaviour exists when the Cr content is less than 10 at.%, while an antiferromagnetic spin ordering appears for Cr contents more than 15 at.%. In the intermediate range between them, short-range antiferromagnetic clusters occur. Nakai *et al* (1987) concluded that the intermediate phase is composed of antiferromagnetic clusters frozen in the matrix of the spin glass, since the cluster size is almost independent of temperature below the freezing temperature of the spins. They also deduced a moment

0953-8984/90/265647 + 10 $03.50

distribution obtained by computer simulation for a two-dimensional triangular lattice containing 40% magnetic atoms. On the other hand, Van Tendeloo *et al* (1985) have observed diffuse maxima at the $1\frac{1}{2}0$ and equivalent positions in the electron diffraction pattern for the disordered Au_4Cr alloy and have interpreted this as being due to the presence of microdomains of the $D0_{22}$ structure and elements of the $D1_a$ structure. Nevertheless, there are no x-ray or neutron diffuse scattering measurements which establish the local atom and spin arrangements in this alloy system.

In this paper we have measured the x-ray diffuse intensities from the disordered Au–20.2, Au–12.6 and Au–8.4 at.% Cr alloys at room temperature, these three specimens having different properties at low temperatures in the magnetic phase diagram. By analysing the diffuse intensity data, we show possible local atomic arrangements, simulated by computer, for the three concentrations. The relationship between local atomic arrangements and spin configurations in these alloys is discussed on the basis of magnetic measurements (Nakai *et al* 1987).

2. Sample preparation

Three single-crystals with different compositions were grown by the Bridgman technique. The purity of the starting materials was 99.99% for both Au and Cr. Plate-like samples of about 10 mm in diameter and 3 mm thick were cut from the ingots. The surface of the samples was parallel to the (210) plane. They were electrically etched with electrolytes of 100 g saturated $CaCl_2$ solution, 73 ml water, 4.5 ml concentrated HCl, 25 ml concentrated $HClO_4$ and 1 g $Cu(NO_3)_2$ to remove the distorted surface layer. The samples were annealed for 18 days at 700 °C and then quenched in ice brine.

The compositions of the three samples were estimated on the basis of the relationship between lattice parameters and composition (Pearson 1967). The compositions were Au–20.2, Au–12.6 and Au–8.4 at.% Cr alloys, respectively.

3. X-ray intensity measurements and data analysis

The x-ray intensity measurements were made by using a four-circle goniometer attached to a rota-unit x-ray generator (RU-300). The incident beam, CuKα radiation, from a Cu target was monochromated by a singly-bent HOPG (highly oriented pyrolitic graphite) crystal.

The diffuse intensity was measured by scanning a volume of reciprocal space at intervals of $\Delta h_i = \frac{1}{20}$ in terms of the distance between the 000 and 200 fundamental diffraction spots and in particular at intervals of $\Delta h_i = \frac{1}{40}$ in the regions where the diffuse maxima have been observed for Au–20.2 at.% Cr. The diffuse scattering intensity distributions are shown on the ($hk0$) reciprocal-lattice plane in Laue units from the samples of Au–20.2, Au–12.6 and Au–8.4 at.% Cr alloys in figures 1(a), (b) and (c), respectively, where the contribution from air scattering has been subtracted. As seen in figure 1, the asymmetry of the diffuse scattering around 110 is not so pronounced that the effect of different atomic sizes for the two species is not serious in the separation of ASRO diffuse scattering from total diffuse scattering. After subtracting both Bragg intensity near the fundamental spots and the contribution from Compton scattering, the measured intensities were converted to absolute units by comparing them with the intensity scattered from polystyrene (C_8H_8) at $2\theta = 100°$ and integrated intensities from

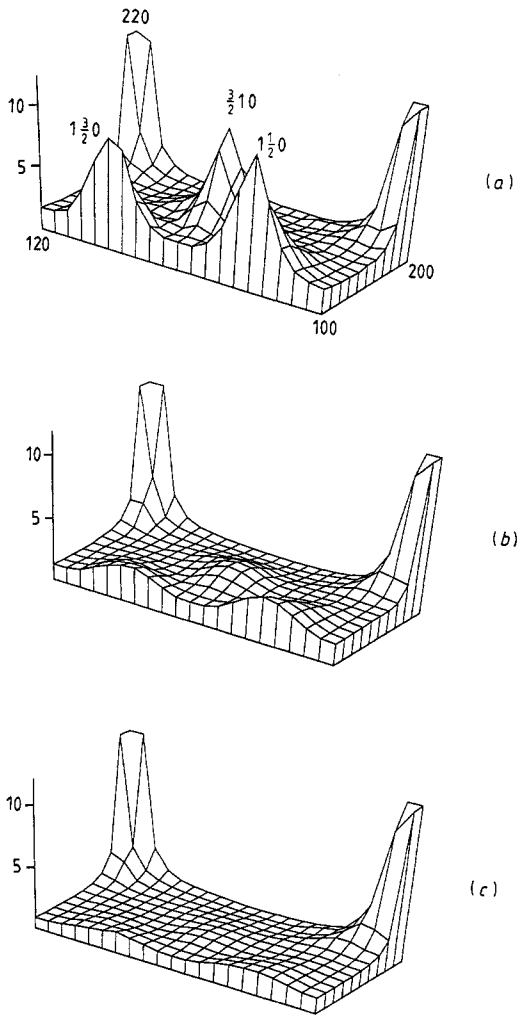

Figure 1. Diffuse scattering intensity distributions on the ($hk0$) reciprocal-lattice plane in Laue units for (*a*) Au–20.2, (*b*) Au–12.6 and (*c*) Au–8.4 at.% Cr alloys.

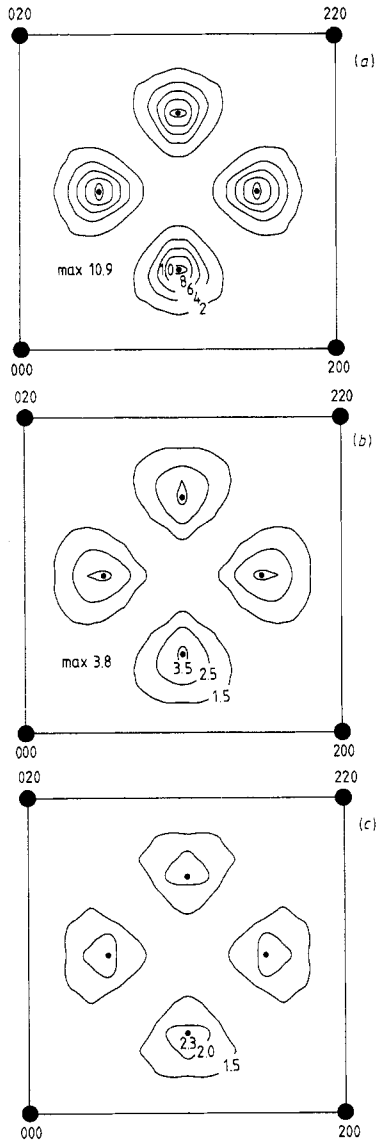

Figure 2. The atomic short-range order components of diffuse scattering in the ($hk0$) plane in Laue units for (*a*) Au–20.2, (*b*) Au–12.6 and (*c*) Au–8.4 at.% Cr alloys.

a powdered Al sample. The conversion factors of these two independent methods agreed within 5%. The ASRO diffuse scattering was obtained by removing the size-effect modulation, as well as Huang scattering and thermal diffuse scattering, from the total diffuse scattering by using the Borie and Sparks method (Borie and Sparks 1971). Intensity distributions due to ASRO are shown in figures 2(*a*), (*b*) and (*c*) for Au–20.2, Au–12.6 and Au–8.4 at.% Cr alloys in Laue units, respectively. Although the position

of diffuse maxima at $1\frac{1}{2}0$ and its equivalent positions does not change with changing Cr content, the absolute values of the diffuse maxima decrease with decreasing Cr content.

4. The ASRO parameter and local atomic arrangement

By Fourier inversion of the ASRO diffuse scattering intensities shown in figure 2, the Warren–Cowley ASRO parameters α_{lmn} were determined up to the 34th shell for the disordered Au–Cr alloys, with an error estimate of less than 10%. They are listed in table 1 and are plotted against the atomic distance r_{lmn} $(= (l^2 + m^2 + n^2)^{1/2})$ in figure 3, where l, m and n are integers. The absolute values of α_{lmn} become smaller with decreasing Cr content. This fact suggests that the ASRO state has a tendency to become more random with decreasing Cr content.

A possible local atomic arrangement could be constructed using the observed ASRO parameters and a simulation program (Suzuki *et al* 1982, Ohshima *et al* 1987). In reproducing the observed ASRO diffuse intensities by this simulation, more than 26th, 17th and 10th shell parameters α_{lmn} were needed for the Au–20.2, Au–12.6 and Au–8.4 at.% Cr alloys, respectively. Thus, the ASRO parameters up to the 31st, 21st and 20th shell α-parameters for the three alloys were adjusted so as to fit the experimentally determined α_{lmn}-values for the atom arrangements of $10 \times 10 \times 10$ FCC unit cells. Both random and tentatively ordered structures were introduced as the initial ones. The final local arrangements of Cr atoms are so similar for the two cases that we adopt the result simulated from the random structure hereafter. The results are shown in figures 4(*a*)–(*f*); (*a*), (*c*) and (*e*) for the ideally random arrangements (RANDOM) in which all the α-parameters are fitted to zero except for $\alpha_{000} = 1$ for Au–20.2, Au–12.6 and Au–8.4 at.% Cr alloys, and (*b*), (*d*) and (*f*) for the observed ASRO structures for Au–20.2, Au–12.6 and Au–8.4 at.% Cr alloys, respectively. In figure 4, only Cr atoms are represented by circles and these are linked together by *red and green solid lines* if they are first- and second-nearest neighbours to each other in a FCC lattice, respectively. A set of α_{lmn} parameters corresponding to the computer-simulated structure is compared with those determined by experiment in table 1. In order to see the agreement between these values and those determined experimentally the ASRO diffuse intensities were reconstructed using α_{lmn}-parameters obtained from the simulated structures. It has been confirmed that the agreement between them is fairly good.

For the Au–20.2 at.% Cr alloy, it is clear that Cr atoms have a preference for lining up along the ⟨1 0 0⟩ direction in figure 4(*b*) for the ASRO structure in comparison with that for the ideally random state in figure 4(*a*). For the Au–12.6 at.% Cr alloy, there is little difference in the structure as seen in figures 4(*b*) and (*d*), indicating that the local atomic arrangement of Cr atoms in the ASRO state deviates from the random state. For the Au–8.4 at.% Cr alloy, the local atomic arrangement of ASRO state in figure 4(*f*) is very similar to that of the ideally random state in figure 4(*e*). To clarify further the obvious difference of arrangements of Cr atoms in these alloys, another structural difference between the ASRO and random states can be characterised by comparing the number of Cr–Cr atom pairs in the first-nearest neighbours and those in the second-nearest neighbours. In table 2 we list these values for the states in the three samples. We see that the number of Cr–Cr atom pairs in the first neighbours is higher in RANDOM than in ASRO, but that the number of Cr–Cr atom pairs in the second neighbours is higher in ASRO than in RANDOM. It can also be seen that the number of Cr–Cr atom pairs both in the first and second neighbours in ASRO approaches that in RANDOM with decreasing Cr content.

Table 1. Atomic short-range order (ASRO) parameters of disordered Au–20.2, Au–12.6 and Au–8.4 at.% Cr alloys determined from the Fourier transform of the ASRO diffuse scattering intensities and those calculated from the model by computer simulation (see figures 4(*b*), (*d*) and (*f*)). *N* is the shell number.

		Au–20.2 at.% Cr		Au–12.6 at.% Cr		Au–8.4 at.% Cr	
N	*lmn*	Exp	Simul	Exp	Simul	Exp	Simul
	000	1.002	1.000	1.001	1.000	1.001	1.000
1	110	−0.155	−0.154	−0.075	−0.075	−0.024	−0.024
2	200	0.198	0.194	0.109	0.109	0.034	0.034
3	211	0.076	0.075	0.027	0.027	0.007	0.007
4	220	−0.081	−0.079	−0.053	−0.052	−0.012	−0.012
5	310	−0.061	−0.061	−0.026	−0.026	−0.010	−0.009
6	222	−0.123	−0.124	−0.061	−0.061	−0.032	−0.032
7	321	0.050	0.050	0.031	0.031	0.019	0.019
8	400	0.131	0.131	0.041	0.042	0.015	0.016
9	330	−0.053	−0.053	−0.028	−0.027	−0.024	−0.023
	411	−0.039	−0.038	−0.010	−0.010	−0.009	−0.009
10	420	0.007	0.006	−0.004	−0.004	−0.005	−0.005
11	332	0.005	0.005	−0.008	−0.008	−0.005	−0.005
12	422	−0.020	−0.020	−0.001	−0.001	−0.007	−0.006
13	431	0.003	0.003	0.006	0.006	0.003	0.003
	510	−0.017	−0.017	−0.001	−0.001	0.001	0.001
14	521	0.019	0.019	−0.001	−0.001	0.004	0.004
15	440	0.023	0.023	0.008	0.008	0.005	0.006
16	433	0.000	0.000	0.002	0.002	0.005	0.005
	530	−0.021	−0.021	−0.004	−0.004	0.001	0.001
17	442	0.005	0.005	−0.006	−0.006	0.003	0.004
	600	0.046	0.047	0.006	0.006	−0.003	−0.002
18	532	−0.001	−0.001	0.002	0.002	−0.001	−0.001
	611	−0.015	−0.015	−0.003	−0.003	0.004	0.004
19	620	0.000	0.000	0.002	0.002	−0.003	−0.003
20	541	−0.006	−0.006	0.002	0.002	−0.002	−0.002
21	622	−0.005	−0.015	−0.011	−0.010	−0.002	—
22	631	0.009	0.009	−0.001	—	−0.002	—
23	444	0.004	0.003	0.007	—	−0.003	—
24	543	−0.004	−0.004	−0.003	—	−0.002	—
	550	0.013	0.013	−0.004	—	−0.001	—
	710	−0.004	−0.005	−0.002	—	−0.003	—
25	640	0.005	0.006	−0.006	—	0.000	—
26	552	0.005	0.005	0.001	—	−0.000	—
	633	0.009	0.009	0.003	—	0.002	—
	721	0.011	0.011	0.006	—	−0.000	—
27	642	0.000	0.000	0.007	—	−0.000	—
28	730	−0.017	−0.017	0.001	—	−0.000	—
29	651	−0.007	−0.007	−0.002	—	−0.001	—
	732	−0.004	−0.004	−0.000	—	0.001	—
30	800	0.026	0.026	0.007	—	0.005	—
31	554	−0.001	—	0.001	—	0.001	—
	741	0.000	—	−0.001	—	0.006	—
	811	−0.008	—	−0.001	—	−0.001	—
32	644	−0.002	—	−0.005	—	−0.000	—
	820	−0.006	—	−0.006	—	0.003	—
33	653	−0.001	—	−0.001	—	0.001	—
34	660	0.003	—	0.004	—	0.010	—
	822	−0.007	—	0.007	—	0.001	—

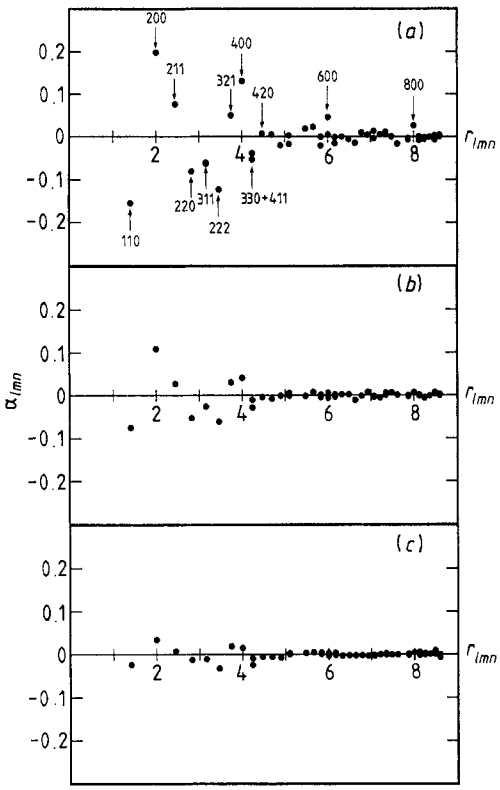

Figure 3. Atomic short-range order parameters α_{lmn} plotted against $r_{lmn} = (l^2 + m^2 + n^2)^{1/2}$ for (*a*) Au–20.2, (*b*) Au–12.6 and (*c*) Au–8.4 at.% Cr alloys.

5. The relation between the ASRO state and the magnetic property

Nakai *et al* (1987) suggested that the origin of the magnetic interaction between Cr atoms is due to an RKKY-type interaction. If we assume that the Fermi wave vector of FCC Au–Cr alloys is close to that of noble metals, then the signs of the first- and second-nearest neighbour interactions are antiferromagnetic and ferromagnetic. Following the previous studies (Suzuki *et al* 1982, Ohshima *et al* 1987), we assigned the spin configuration of the ground state to the Cr network in figure 4 where an Ising spin system is introduced for simplicity. Several types of clusters are found to exist and these are connected to one another by antiferromagnetic coupling for first-nearest neighbours. However, frustrated Cr atoms (with respect to spin configuration) linked by antiferromagnetic coupling on one side and by ferromagnetic coupling on the other side are occasionally seen. In table 2, we show the values for a regular triangle lattice connecting with Cr–Cr atom pairs in the first-nearest neighbours for the two states of the three samples, and the ratio number of this for ASRO to that for RANDOM. The number of such a frustrated triangular lattice decreases as ASRO develops, and its ratio also decreases with increasing Cr content. These facts are considered to affect the magnetic properties of Au–Cr alloys. At low temperatures in the magnetic phase diagram, Nakai *et al* (1987) reported that the 20.2 at.% Cr alloy lies in the antiferromagnetic state region, that that of the 8.4 at.% Cr alloy lies in the spin-glass region and that that of the 12.6 at.% Cr alloy shows short-range antiferromagnetic clusters. Therefore, it can be said that the spin-glass state

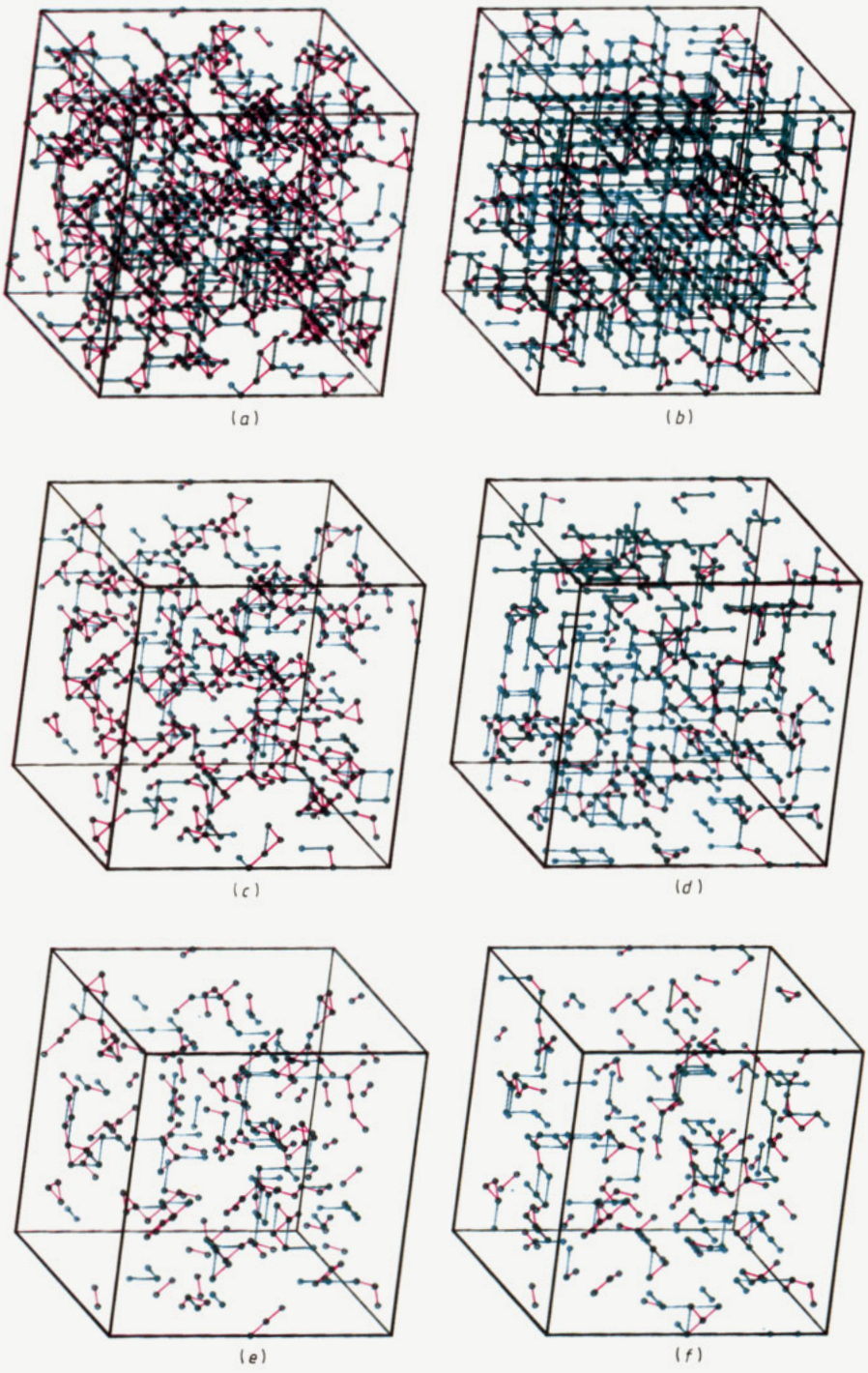

Figure 4. Three-dimensional distributions of Cr atoms simulated on 10 × 10 × 10 FCC unit cells; (*a*), (*c*) and (*e*) for the ideally disordered state of Au–20.2, Au–12.6 and Au–8.4 at.% Cr alloys, respectively, and (*b*), (*d*) and (*e*) for the observed ASRO structures of the same alloy compositions. Only Cr atoms are represented by circles and these are linked together by *red and green solid lines* to their first- and second-nearest neighbours in a FCC lattice.

Table 2. The number of Cr–Cr atom pairs in the (i) first- and (ii) second-nearest neighbours, (iii) the number of regular triangle lattices connected with the first-nearest neighbours, and (iv) the ratio number of this for ASRO to that for RANDOM.

	Au–20.2 at.% Cr		Au–12.6 at.% Cr		Au–8.4 at.% Cr	
	RANDOM	ASRO	RANDOM	ASRO	RANDOM	ASRO
(i)	1034	404	409	195	186	134
(ii)	489	888	192	350	84	123
(iii)	259	9	62	3	16	6
(iv)	0.037		0.048		0.375	

appears if the Cr atoms in the alloy become more random and that magnetic ordering is observed if the Cr atoms have a preference to ordering. Furthermore, it may be considered that the number of frustrated triangle lattices in an alloy affects the driving force to a spin-glass or antiferromagnetic state. We will consider whether this idea is applicable to the case of other alloy systems, for example, Au–Mn, Ag–Mn and Cu–Mn (Koga *et al* 1990).

Acknowledgments

The authors wish to thank Professor J Harada of Nagoya University for helpful discussions. The present work was supported in part by the University of Tsukuba Project Research.

References

Borie B and Sparks C J 1971 *Acta Crystallogr.* A **27** 198
Koga K, Ohshima K and Harada J 1990 in preparation
Nakai Y, Sakuma M and Kunitomi N 1987 *J. Phys. Soc. Japan* **56** 301
Ohshima K, Iwao N and Harada J 1987 *J. Phys. F: Met. Phys.* **17** 1769
Pearson W B 1967 *A Handbook of Lattice Spacings and Structures of Metals and Alloys* (Oxford: Pergamon) p 653
Suzuki H, Harada J, Matsui M and Adachi K 1982 *Acta Crystallogr.* A **38** 522
Van Tendeloo G, Amelinckx S and de Fontaine D 1985 *Acta Crystallogr.* B **41** 281